Journal of Crohn's and Colitis, 2023, **17**, 804–815
https://doi.org/10.1093/ecco-jcc/jjac194
Advance access publication 26 December 2022
Original Article

Mass-Cytometry-Based Quantification of Global Histone Post-Translational Modifications at Single-Cell Resolution Across Peripheral Immune Cells in IBD

Lawrence Bai,[a,*] Denis Dermadi,[b,c,*] Laurynas Kalesinskas,[d,*] Mai Dvorak,[b,e] Sarah E. Chang,[b,e] Ananthakrishnan Ganesan,[f] Samuel J. S. Rubin,[g] Alex Kuo,[b,e] Peggie Cheung,[b,e] Michele Donato,[b,c] Paul J. Utz,[a,b,e,†] Aida Habtezion,[a,b,g,†] Purvesh Khatri[a,b,c,†]

[a]Immunology Program, Stanford University School of Medicine, 1215 Welch Road, Modular B, Stanford, CA 94305, USA
[b]Institute for Immunity, Transplantation and Infection, School of Medicine, Stanford University, Stanford, CA 94305, USA
[c]Center for Biomedical Informatics Research, Department of Medicine, Stanford University, Stanford, CA 94305, USA
[d]Biomedical Informatics Training Program, Stanford University School of Medicine, 1265 Welch Road, MSOB X-343, Stanford, CA 94305, USA
[e]Division of Immunology and Rheumatology, Department of Medicine, Stanford University School of Medicine, Stanford, CA 94305, USA
[f]Computational and Mathematical Engineering, Stanford University, 475 Via Ortega, Suite B060, Stanford, CA 94305, USA
[g]Division of Gastroenterology and Hepatology, Department of Medicine, Stanford University School of Medicine, Stanford, CA 94305, USA

Corresponding author: Purvesh Khatri, Immunology Program, Stanford University School of Medicine, 1215 Welch Road, Modular B, Institute for Immunity, Transplantation and Infection, School of Medicine, Stanford University, Center for Biomedical Informatics Research, Department of Medicine, Stanford University, Stanford, CA 94305, USA. Email: pkhatri@stanford.edu
*These authors contributed equally
†Co-senior authors

Abstract

Background and Aims: Current understanding of histone post-translational modifications [histone modifications] across immune cell types in patients with inflammatory bowel disease [IBD] during remission and flare is limited. The present study aimed to quantify histone modifications at a single-cell resolution in IBD patients during remission and flare and how they differ compared to healthy controls.

Methods: We performed a case-control study of 94 subjects [83 IBD patients and 11 healthy controls]. IBD patients had either ulcerative colitis [$n = 38$] or Crohn's disease [$n = 45$] in clinical remission or flare. We used epigenetic profiling by time-of-flight [EpiTOF] to investigate changes in histone modifications within peripheral blood mononuclear cells from IBD patients.

Results: We discovered substantial heterogeneity in histone modifications across multiple immune cell types in IBD patients. They had a higher proportion of less differentiated $CD34^+$ haematopoietic progenitors, and a subset of $CD56^{bright}$ natural killer [NK] cells and γδ T cells characterized by distinct histone modifications associated with gene transcription. The subset of $CD56^{bright}$ NK cells had increases in several histone acetylations. An epigenetically defined subset of NK cells was associated with higher levels of C-reactive protein in peripheral blood. $CD34^+$ monocytes from IBD patients had significantly decreased cleaved H3T22, suggesting they were epigenetically primed for macrophage differentiation.

Conclusion: We describe the first systems-level quantification of histone modifications across immune cells from IBD patients at a single-cell resolution, revealing the increased epigenetic heterogeneity that is not possible with traditional ChIP-seq profiling. Our data open new directions in investigating the association between histone modifications and IBD pathology using other epigenomic tools.

Key Words: Single-cell epigenetic; histone modifications; inflammatory bowel disease; crohn's disease; ulcerative colitis

1. Introduction

The incidence and prevalence of inflammatory bowel diseases [IBD], which affect more than 6.8 million patients globally, is rising worldwide.[1,2] Broadly, IBD comprises two types of chronic relapsing and remitting inflammatory intestinal disorders: [1] ulcerative colitis [UC] and [2] Crohn's disease [CD]. UC is characterized by mucosal inflammation, starting from the rectum, that can extend to the entire colon.[3] In contrast, CD can affect any part of the gastrointestinal tract, and disease lesions can present as ulcers or strictures or penetrate from the lumen to the fat surrounding the intestines.[4] Most patients are diagnosed in late adolescence/early adulthood, and curative therapies do not exist, leading to compounding prevalence.[5,6] Current treatments aim to induce and maintain clinical and endoscopic remission. The lack of curative therapies and the undesirability of intestinal inflammation underline the need for novel medication options for patients with IBD.

Multiple factors contribute to the pathophysiology of IBD, including genetic susceptibility, microbial and immunological factors, and environmental influences.[7] Family history remains the strongest risk factor for IBD and is reported in about 8–12% of patients with IBD.[8] However, despite multiple large-scale genome-wide association studies [GWAS], genetic variation thus far only explains about 8.2–13.1% of disease heritability.[9] Recent epidemiological studies have pointed

© The Author(s) 2022. Published by Oxford University Press on behalf of European Crohn's and Colitis Organisation.
This is an Open Access article distributed under the terms of the Creative Commons Attribution-NonCommercial License (https://creativecommons.org/licenses/by-nc/4.0/), which permits non-commercial re-use, distribution, and reproduction in any medium, provided the original work is properly cited. For commercial re-use, please contact journals.permissions@oup.com

to the increasing importance of environmental triggers for inducing IBD,[10] suggesting epigenetics may play an important role in IBD. Epigenetic modifications can change gene expression patterns without altering the underlying DNA sequence.[11] Epigenetic modifications on DNA or histones alter chromatin structure, which can substantially impact transcriptional priming, activation and repression. These semi-permanent changes can be induced by external or environmental changes, including pollutants, smoking and diet.[12,13] Thus, epigenetics provides a potential mechanistic connection between genetic predisposition and environmental triggers in the pathology and pathogenesis of IBD.[14–16] Recent studies have begun to uncover several molecular modalities of epigenetics and their contributions to IBD, including DNA methylation,[17–20] histone modifications[21–23] and microRNAs [miRNAs].[24,25] For instance, histone deacetylation dysregulation or inhibition has ameliorated experimental IBD *in vivo*.[26,27] Further, although a few studies have identified histone modification signatures in intestinal epithelial cells [IECs] of patients with IBD,[23] there is little data on how these modifications change across the numerous immune cells during disease flare and progression.

Here, we used the recently described mass cytometry-based technique for epigenetic profiling, called EpiTOF,[28] to profile the abundance of 38 histone post-translational modifications [histone modifications], histone variants and histone-modifying enzymes at a single-cell level across 22 immune cell subsets from 83 patients with IBD and 11 healthy controls. We investigated histone modifications in peripheral blood mononuclear cells [PBMCs] that may inform local tissue immune responses under disease conditions. Using EpiTOF, we identified changes in histone modifications, including acetylation, methylation and ubiquitination at a single-cell level in multiple haematopoietic cell types from patients with IBD, many of which have not been previously described in the context of IBD. We found changes in histone modifications in $CD34^+$ haematopoietic progenitor cells [HPCs], natural killer [NK] cells, γδ T cells and classical monocytes. Our study provides a unique resource to pinpoint specific cell type–histone modification pairs that are dysregulated in patients with IBD. Importantly, our findings support a role for histone modifications in IBD pathology, specifically in haematopoietic progenitors, NK and γδ T cells. Our study identifies several histone modifications that should be further investigated using ChIP-seq, ATAC-seq, cut&tag, etc., to understand the upstream and downstream programmes associated with epigenomic state changes at the global cellular level, and whether they play any causal roles in IBD pathology.

2. Methods

2.1 Patient samples

All blood samples were collected using a study protocol approved by the Stanford Institutional Review Board. Informed consent was obtained from subjects aged 21–65 years with an IBD-specializing gastroenterologist-confirmed diagnosis of IBD [except healthy controls], excluding those who were pregnant, had other autoimmune or inflammatory diseases [except for extraintestinal manifestations of IBD], malignancy, active infection at the time of enrolment, underwent surgery within 6 months of enrolment, had a blood transfusion within 6 months of enrolment, received an organ or bone marrow transplant or were unable to provide informed consent. All clinical data for subjects were current at the time of sample collection. IBD flare was determined by IBD-specializing physicians for the standard of care and intent to treat using all available information, including bloodwork, clinical assessments, patient history and/or endoscopy. When available [for most patients], recent endoscopy reports were reviewed to confirm the disease state.

2.2 Blood leukocyte isolation and cryopreservation

Blood samples were collected by the standard of care venipuncture; three vacutainers with sodium heparin [BD, cat. #366480] were filled with blood and kept at room temperature until processing, which occurred within 2 h. Blood was centrifuged in vacutainers used for collection at 2000 r.p.m. for 10 min. Plasma was aspirated from the top and frozen at −80°C in 1-mL aliquots in cryovials [Thermo Fisher Scientific, cat. #375418] using a freeze controller [Bel-Art Products, cat. #F18844-0000] pre-chilled to −4°C according to the manufacturer's instructions. The remaining blood was diluted 1:1 in PBS without calcium or magnesium, layered over 15 mL of Ficoll-Paque [GE Healthcare, cat. #17-1440-03] in an Accuspin tube [Sigma-Aldrich, cat. #A2055] and centrifuged at 2000 r.p.m. for 20 min at 21°C with acceleration at five and break at zero. The buffy coat leukocyte layer was collected and washed twice in 50 mL of PBS without calcium or magnesium by centrifuging at 2000 r.p.m. for 10 min. Cells were counted, washed again and resuspended in Recovery Cell Culture Freezing Medium [Thermo Fisher Scientific, cat. #12648010] at 4.5–11 × 10^6 cells/mL in 1-mL aliquots, transferred to a freeze controller [Bel-Art Products, cat. #F18844-0000] pre-chilled to −4°C according to the manufacturer's instructions, stored at −80°C for 1–2 weeks, and then transferred to liquid nitrogen for storage.

2.3 Lanthanide labelling of antibodies for mass cytometry

Antibodies were conjugated with the lanthanides as previously described[28] using a MAXPAR antibody labelling kit [Fluidigm], following the manufacturer's protocol. All antibodies were validated for specificity previously, and documents are publicly available online [https://www.cell.com/cms/10.1016/j.cell.2018.03.079/attachment/cd51ab10-c003-4073-8a66-63e9180110e9/mmc4.pdf].[28] TCEP [ThermoFisher] was added in 100-fold molar excess to generate sulphhydryl groups for maleimide-mediated conjugation of metal-chelating polymers. Conjugated antibodies were diluted in antibody stabilizing solution [Boca Scientific] containing 0.05% sodium azide [Sigma] for storage.

2.4 Mass cytometry [sample processing, staining, barcoding and data collection]

Preparation of samples for mass cytometry was done as previously described.[28] Briefly, cryopreserved PBMCs were thawed and incubated in RPMI 1640 media [ThermoFisher] containing 10% FBS [ATCC] at 37°C for 1 h before processing. Cisplatin [ENZO Life Sciences] was added to 10 μM final concentration for viability staining for 5 min before quenching with CyTOF Buffer (PBS [ThermoFisher] with 1% BSA [Sigma], 2 mM EDTA [Fisher], 0.05% sodium azide). Cells were centrifuged at 400 *g* for 8 min and stained with lanthanide-labelled antibodies against immunophenotypic markers in CyTOF buffer containing Fc receptor blocker [BioLegend] for 30 min at room temperature. Following extracellular marker staining,

cells were washed three times with CyTOF buffer and fixed in 1.6% PFA [Electron Microscopy Sciences] at 1 × 10^6 cells/mL for 15 min at room temperature. Cells were centrifuged at 600 *g* for 5 min post-fixation and permeabilized with 1 mL ice-cold methanol [Fisher Scientific] for 20 min at 4°C. Then, 4 mL of CyTOF buffer was added to stop permeabilization followed by two PBS washes. Mass-tag sample barcoding was performed following the manufacturer's protocol [Fluidigm]. Individual samples were combined and stained with intracellular antibodies in CyTOF buffer containing Fc receptor blocker [BioLegend] overnight at 4°C. The following day, cells were washed twice in CyTOF buffer and stained with 250 nM 191/193Ir DNA intercalator [Fluidigm] in PBS with 1.6% PFA for 30 min at room temperature. Cells were washed twice with CyTOF buffer and once with double-deionized water [ddH_2O] [ThermoFisher], followed by filtering through a 35-µm strainer to remove aggregates. Cells were resuspended in ddH_2O containing four element calibration beads [Fluidigm] and analyaed on CyTOF2 [Fluidigm]. Raw data were concatenated and normalized using calibration beads following the manufacturer's protocol for downstream processing.

2.5. Data pre-processing, normalization and visualization

Raw data were pre-processed using FlowJo [FlowJo, LLC] to identify cell events from individual samples using palladium-based mass tags and segregate specific immune cell populations by immunophenotypic markers. A detailed gating hierarchy is described in Supplementary Figure 1. For downstream computational analyses, single-cell data for immune cell subtypes from individual subjects were exported from FlowJo. Exported pre-processed files were analysed using R. Technical batch effects were corrected using quantile normalization across each cell surface or epigenetic marker measured in each panel. Epigenetic marks were normalized by their histone H3 and H4 levels using the sample-based normalization method previously described.[29] All data visualization graphs and plots were generated using R [version 3.6.3].

2.6 Statistical analysis

To account for inherent immune cell proportion biases in PBMCs, we subsampled 9000 cells per cell type across all runs [~200 000 total cells per analysis]. We performed UMAP [Uniform Manifold Approximation and Projection] analysis using all measured epigenetic modification markers or cell surface markers as feature inputs [Figure 1; Supplementary Figure 2]. For cell-type-specific UMAP analyses, we used the maximum between 120 000 cells or the total number of cells measured of that specific cell type. All UMAP analyses were performed using the *uwot* package [version 0.1.10] for the acetylation panel [Panel A] and methylation panel [Panel M]. We used the *Rphenoannoy* package [version 0.1.0] for the unsupervised clustering of cells.

To address the sample size restriction of EpiTOF mass-tag barcoding, we integrated healthy subjects from previous studies[28,30] to increase statistical power. To show that healthy individuals from previous studies are epigenetically comparable to the healthy controls in this study, we sampled single cells across healthy subjects from previous and current studies to perform UMAP. We found no differences between the healthy controls from different studies [Supplementary Figure 6A and B]. We then integrated ten randomly selected meta-samples [N = 5; S = 10] for each dataset before calculating subject-level data as done previously.[28] We calculated the mean of single-cell normalized values for each cell type–epigenetic mark pair to obtain 836 unique cell–mark pair features per sample. We then computed effect size differences for each dataset and compared each biologically relevant pairwise comparison, correcting for multiple hypotheses (false discovery rate [FDR] < 0.05). We compared the cell type–histone modification values between meta-samples and *t*. We found very high *r* coefficients for both the mean abundance and the variance, suggesting that these meta-samples are highly consistent with healthy subjects.

To estimate immune cell proportions in publicly available IBD gene expression datasets, we performed cell-mixture deconvolution using the immunoStates[31] matrix in the MetaIntegrator[32] package [version 2.1.5]. Total histone acetylations are defined as the sum of abundances of individual histone acetylations [H3K9ac, H3K14ac, H3K18ac, H3K23ac, H3K27ac, H3K56ac, H4K5ac, H4K16ac, H2BK5ac] within each immune cell type.

Since cells exist along a continuous developmental spectrum, we reasoned that trajectory inference analysis using epigenetic data would reveal non-linear relationships between epigenetic marks, which can be overlooked in conventional clustering analysis. We adapted a trajectory mapping algorithm [tSpace[33]] to run an analysis on multiple immune cell types to uncover these relationships. We analysed the maximum of 120 000 cells, or the total cells measured for each cell type. Because the epigenetic trajectories were circular, we then linearized each trajectory using the 'periodic_lowess' option in the *princurve* package [version 2.1.6] to investigate cell subpopulation changes along the trajectory. For each analysis, cells were binned, and cell proportions were calculated for each bin along the trajectory. All statistical analyses were performed using R [version 3.6.3].

We built a linear classification model using the *caret* package in R [version 6.0-86]. We performed logistic regression with 5-fold cross-validation over 50 iterations to ensure that the area under the curve [AUC] of the model was robust.

3. Results

3.1 Study design

We enrolled 83 patients with gastroenterologist-confirmed IBD and 11 healthy volunteers [Table 1]. IBD samples included subjects with UC [*n* = 38] or CD [*n* = 45] in clinical remission or flare [Figure 1A; Supplementary Table 1]. We matched the disease-group demographics as closely as possible for age and sex. Disease phenotypes were specific to each diagnosis and could not be matched. We profiled 18.4 million cryopreserved leukocytes isolated from peripheral blood by EpiTOF using 16 cell surface antigens, two histone proteins [total H3 and H4], and 38 histone modification epitopes across two panels of lanthanide-labelled antibodies as described before[34] [Supplementary Table 2].

3.2 Single-cell analysis of EpiTOF reveals epigenetic heterogeneity of peripheral immune cells in patients with IBD

We used UMAP[35] to visualize EpiTOF single-cell data in the acetylation and methylation panels across all cell types in lower dimensions [see Methods]. While the phenotypic cell markers showed immune cells clustered as expected for

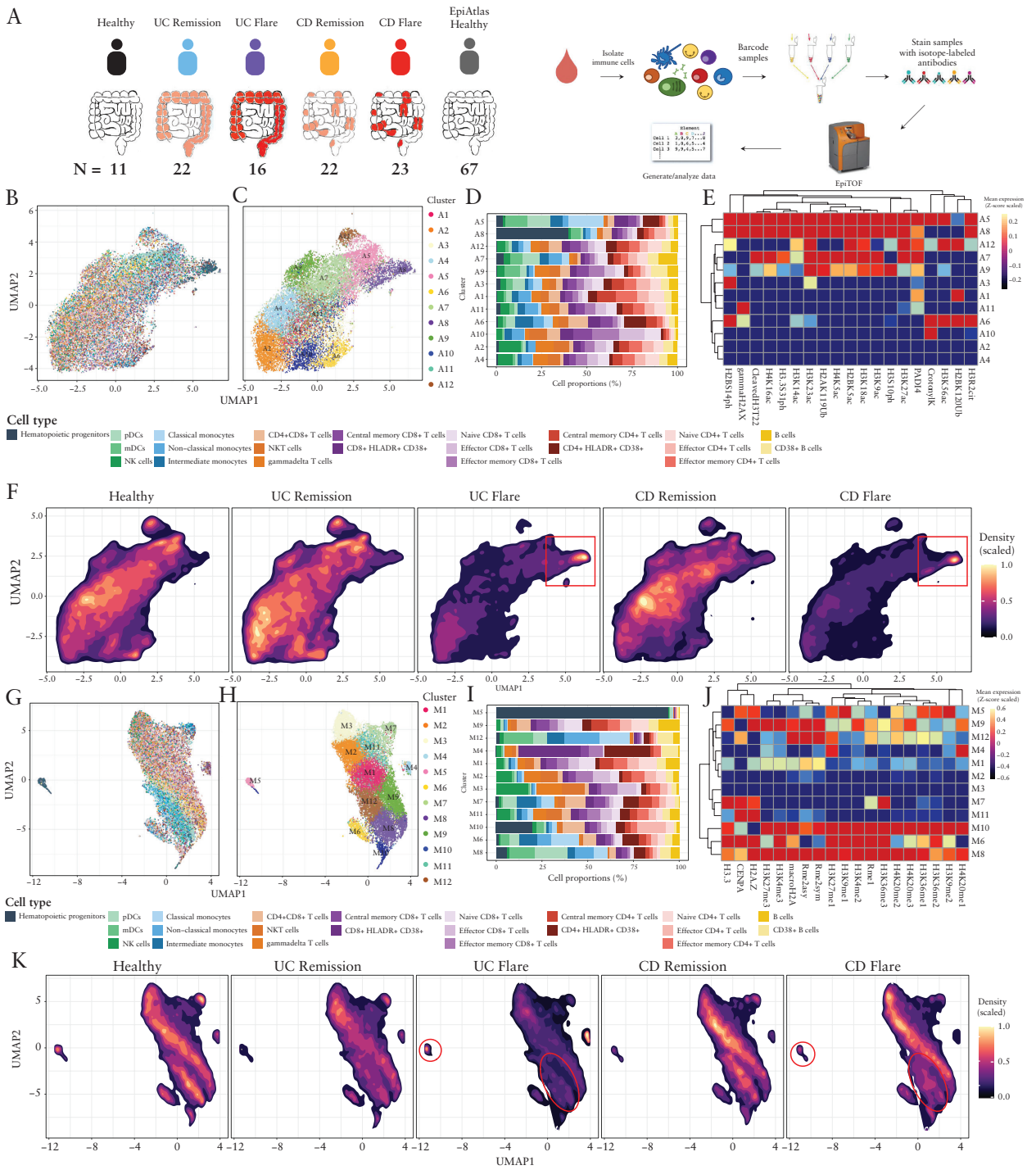


Figure 1. EpiTOF reveals unique epigenetic clusters altered in patients with IBD. [A] Cohort definition and experimental design of EpiTOF. For each sample, we collected data across two antibody panels: [B–F] histone acetylation and [G–K] histone methylation, and used UMAP to investigate single-cell changes between IBD and healthy controls [see Methods]. [B, G] Single-cell UMAP coloured by cell type identity. [C, H] Unsupervised clustering using Phenograph. [D, I] Immune cell type proportions for each identified cluster. [E, J] Mean expression of histone modification abundances for each cell cluster [scaled]. [F, K] Cell density plots separated by disease condition.

both panels [Supplementary Figure 2], histone modifications mostly separated CD34⁺ HPCs, and myeloid- and lymphoid-lineage cells in both panels independent of cell surface marker abundance [Figure 1B and G; Supplementary Figures 3 and 4]. Unsupervised clustering using only histone modification values with Phenograph[36] found 12 clusters in the acetylation [clusters A1–A12] and methylation panels [clusters M1–M12] [Figure 1C and H]. Unlike clustering using cell surface phenotypic markers, each cluster using histone modifications included all immune cell types, demonstrating shared epigenetic heterogeneity in each immune cell type [Figure 1D and I]. Clusters A8 and M5 were predominantly composed of CD34⁺ HPCs, whereas cluster M4 was predominantly composed of HLA-DR⁺CD38⁺CD4 and CD8 T cells. Average histone modification abundance within each cluster further demonstrated broad epigenetic heterogeneity. Almost all histone

Table 1. Summary demographics of IBD patients and healthy subjects

	Healthy	UC	CD	EpiAtlas Healthy
Diagnosis [no. of patients]	11	38	45	67
Disease status [remission/flare]	n/a	22/16	22/23	n/a
Sex [F/M]	6/5	16/22	19/26	35/32
Age (median years [range])	41 [27–63]	37 [21–65]	36 [22–65]	35 [21–65]
Age at onset (median years [range])	n/a	25.665 [5–65]	21.5 [3–53]	n/a
Disease duration (median years [range])	n/a	8.5 [0–45]	12 [1–39]	n/a
Reported extraintestinal manifestations [no. of patients]	n/a	10	18	n/a
Crohn's disease phenotype				
	CD			
Location [no. of patients]				
Ileum only	2			
Ileum and colon	28			
Colon only	12			
Behaviour [no. of patients]				
Inflammatory	13			
Stricturing	13			
Penetrating	6			
Reported perianal disease [no. of patients]	11			
Ulcerative colitis phenotype				
	UC			
Location [no. of patients]				
Left-sided	7			
Pan colonic	24			
Proctitis	4			

modifications were higher in clusters A5, A8, M8 and M10 [Figure 1E and J] and lower in clusters A2, A4, A10, M2 and M3 [Figure 1E and J]. In the methylation panel, this could be explained in part by the ratio of repressive [H3K27me3] versus active [H3K36me3] histone modifications, where lymphoid cells had a higher ratio [>1] compared to myeloid cells [<1] [Supplementary Figure 5A, D, H]. Collectively, these results demonstrate pronounced epigenetic heterogeneity of immune cells in patients with IBD.

3.3 CD34⁺ progenitors from patients with IBD undergoing flare are epigenetically less differentiated

While CD34⁺ HPCs in patients with IBD were enriched in cluster A8 from the acetylation panel [Figure 1F], they were depleted in cluster M8 from the methylation panel [Figure 1K] compared to healthy controls. Patients with IBD had a significantly higher proportion of CD34⁺ HPCs in cluster A8 than healthy controls, irrespective of disease severity [Figure 2A and B]. CD34⁺ HPCs in cluster A8 had a significantly higher abundance of H4K16ac, cleaved H3T22, H3K14ac and H3.3S31ph compared to CD34⁺ HPCs not in cluster A8 [Figure 2C and D]. Decreased H4K16ac in human CD34⁺ HPCs reduces colony-forming potential, a proxy for stem cell activity.[37] Similarly, reduced H3K14ac levels in mice led to the loss of haematopoietic stem cells [HSCs][38] and leukaemia stem cells [LSCs].[39] These studies suggest that the higher histone acetylation marks in cluster A8 are essential for HPC maintenance and may act as epigenetic markers of these cells. Hence, these results suggest that less differentiated CD34⁺ HPCs are in higher proportion in peripheral blood from patients with IBD, irrespective of remission or flare.

Similarly, when using the methylation panel, CD34⁺ HPCs also formed distinct clusters, where one subset [M5] was distinct from other CD34⁺ HPCs in clusters M8 and M10 [Figure 1H and I]. Therefore, we re-embedded only CD34⁺ HPCs using the histone modifications profiled as part of the methylation panel, which confirmed the presence of two distinct cell subclusters, HPC1 and HPC2 [Figure 2E]. Patients with IBD had a significantly higher proportion of CD34⁺ HPCs in HPC1, but there was no difference between patients in clinical remission or flare [Figure 2E and F]. HPC1 had significantly lower levels of H3K9me2 and higher levels of asymmetric and symmetric arginine dimethylation [Rme2asy, Rme2sym] compared to HPC2 [Figure 2G and H]. Previous studies have shown that decreased H3K9me2 levels promote more stem-cell-like properties in CD34⁺ HPCs,[40] whereas conditional knockouts of Rme2asy and Rme2sym arginine residues reduced the number of HPCs.[41,42] The HPC1 cluster, enriched in progenitor cells from patients with flares, was associated with increased blood C-reactive protein [CRP], a marker of active inflammation [Figure 2I]. Our findings demonstrate that progenitors enriched in histone methylations [HPC1] are associated with inflammation in the gut, as observed through increased CRP. Our results suggest progenitors from patients with IBD epigenetically reprogram due to inflammation, supporting growing evidence of stem cell inflammatory modulation.

Given that HPCs are post-mitotic cells in the blood, it is important to note that they do not divide but only transcribe

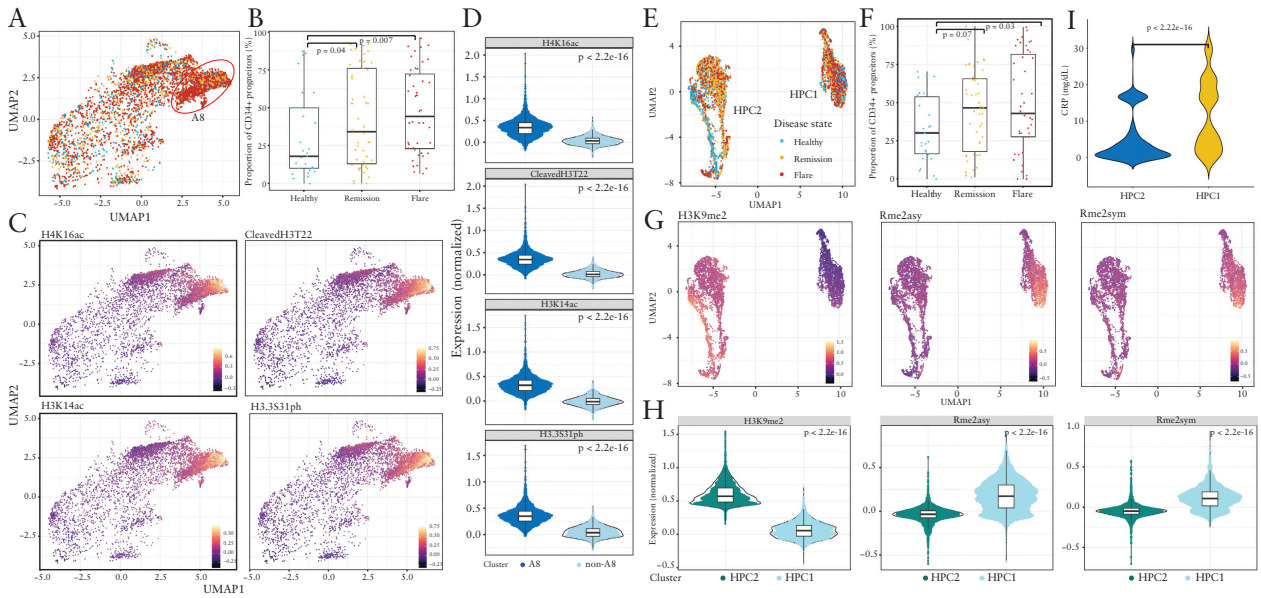


Figure 2. Altered histone modification abundances in CD34⁺ HPCs from patients with IBD. HPC-specific UMAP of [A] acetylation panel or [E] methylation panel. Boxplots of HPC proportions in A8 [B] or HPC1 [F] between patients undergoing flare, in remission or healthy controls. Scatterplots and violin plots of the most differentially abundant histone modifications between cluster A8 and non-A8 HPCs [C, D] or HPC1 and HPC2 [G, H]. [I] Violin plots of CRP blood concentration across HPC cell clusters.

essential gene programmes needed to support their circulation in the blood. Thus, observed differences between healthy and IBD patients may reflect impaired differentiation of CD34⁺ progenitors in the bone marrow and inflammation-induced transcriptional activity.

3.4 Subject-level comparison of immune cell–histone modification pairs identifies epigenetic changes in NK cells from patients with IBD

We sought to investigate subject-level epigenetic differences between healthy controls and patients with UC or CD. To increase statistical power, we utilized 67 age- and sex-matched healthy subjects from our previous studies[28,30] by repeatedly sampling them [see Methods]. We found that the epigenetic profiles of these healthy subjects were highly similar to the healthy subjects in the current study, and there were no batch effects [Supplementary Figure 6; see Methods]. We then used the aggregated mean values for each cell type–histone modification pair per sample and calculated effect sizes for each biologically relevant pairwise group comparison. After multiple hypotheses correction, 70 histone modifications–immune cell pairs were statistically significantly different in patients with CD or UC compared to healthy controls [FDR ≤ 5%; Figure 3A].

Five histone modifications [H2BK5ac, H3K36me1, H3K4me3, macroH2A and Rme2sym] and PADI4 in NK cells were significantly higher in patients with CD compared to healthy controls [Supplementary Figure 7]. We created an epigenetic trajectory of NK cells using tSpace, a graph-based trajectory algorithm, to identify potential non-linear relationships between NK cells and epigenetic markers in the context of IBD. Analysis of methylation profiles of NK cells using tSpace revealed a circular trajectory [Figure 3B]. Visual inspection of cell density along the trajectory suggested a shift of NK cells in CD as well as UC flare [Figure 3C]. We further investigated this observation by linearizing the trajectory, identifying subclusters, and calculating cell proportions in each subcluster [Figure 3D and E; see Methods]. Cluster NK1 contained a higher proportion of NK cells from all IBD patient subsets, particularly from patients with CD, with higher levels of almost all methylation markers. NK cells in this cluster were $CD56^{bright}CD16^{low}$, which are conventionally defined as $CD56^{bright}$ cytokine-producing NK cells[43] [Figure 3E and F]. While each NK cell subset had a distinct epigenetic profile, histone modification abundance was not significantly different when comparing disease conditions within each subset [Supplementary Figure 8]. This suggests that the subject-level differences observed in histone modifications in NK cells between CD and healthy controls are probably driven by the cell proportion differences in the NK cell subpopulations between healthy controls and patients with UC or CD.

Indeed, the proportions of NK cells in peripheral blood from patients with IBD were increased compared to healthy controls, especially the $CD56^{bright}$ subset. Furthermore, the NK1 cluster was associated with high CRP in the blood [Figure 3G]. Importantly, the NK1 cluster was enriched for histone modifications associated with active gene transcription, further providing a link between active inflammation and active gene transcription in immunomodulatory NK cells. We found that NK cells in cluster NK1 had higher abundances of H3K4me3, H3K36me1 and Rme2sym [Figure 3A]. H3K4me3 is a well-studied histone modification often associated with transcription start sites of actively transcribed genes.[44] In patients with CD, intestinal epithelial cells have altered H3K4me3 peak levels at genes involved in immunoregulation.[23] H3K36 monomethylation [H3K36me1] is considered an initial modification that can lead to H3K36 di- [H3K36me2] and trimethylation [H3K36me3], whose roles vary but can be involved in transcriptional activation and maintenance.[45,46] Symmetric arginine demethylation via the methyltransferase *PRMT5* is necessary for T and NK cell maintenance, as well as initiation of Type I and III interferon signalling.[47,48] Taken together, these results suggest that circulating NK cells from patients with IBD are associated with

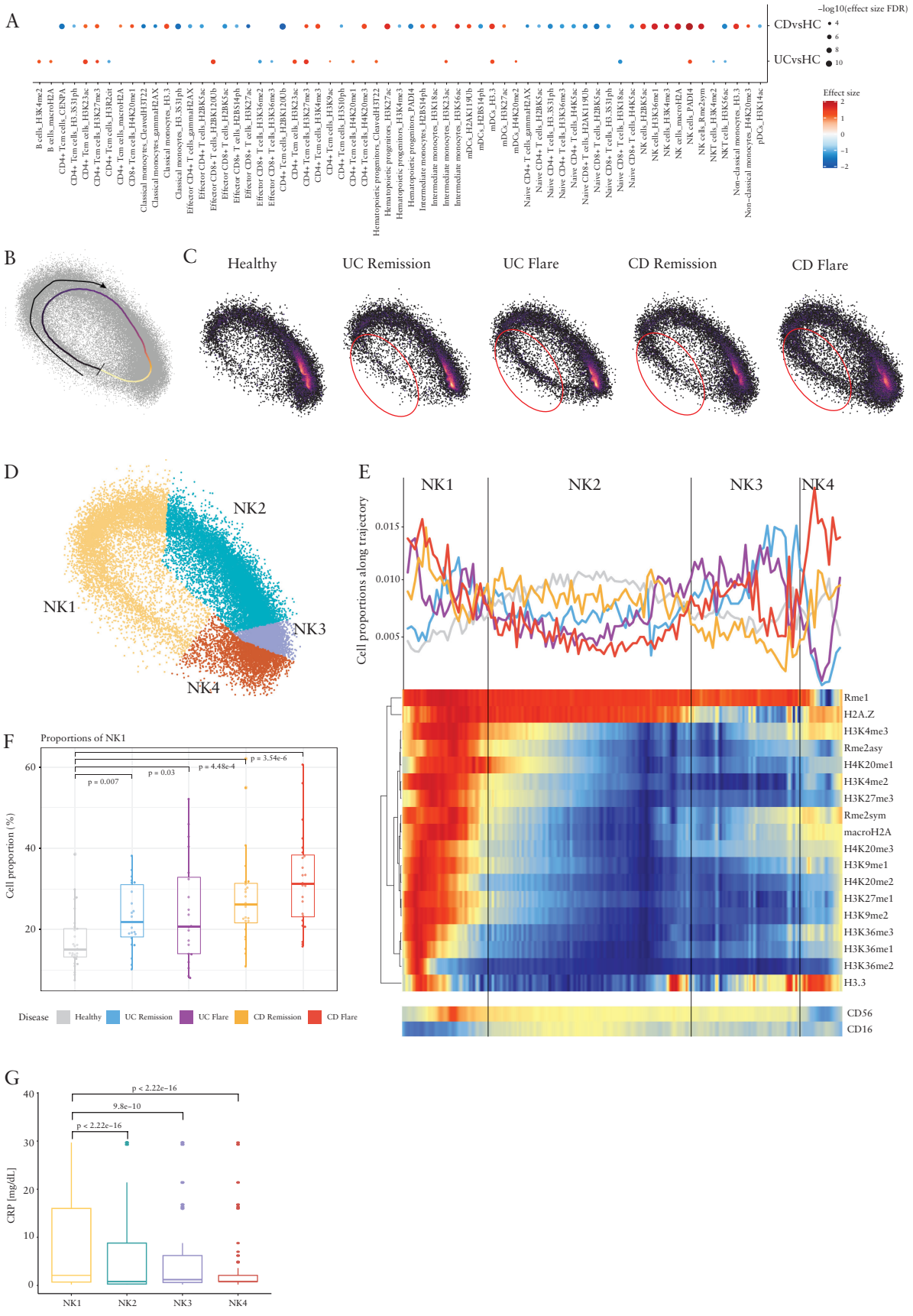


Figure 3. Epigenetic shifts in NK cells from patients with IBD. [A] Circle heatmap of effect size differences of cell type–histone modification pairs between CD or UC vs. healthy controls. [B] tSpace trajectory analysis of EpiTOF histone modification abundance in NK cells, separated by disease condition [C]. [D] Clustering of NK cells along the tSpace trajectory. [E] Line plots of relative cell proportions between each disease condition along the linearized trajectory [top]; heatmap of histone modification abundance or cell surface marker expression across the linearized trajectory [bottom]. [F] Boxplot of NK1 cell proportions across disease conditions. [G] Boxplot of CRP blood concentration across NK cell clusters; Student's *t*-test.

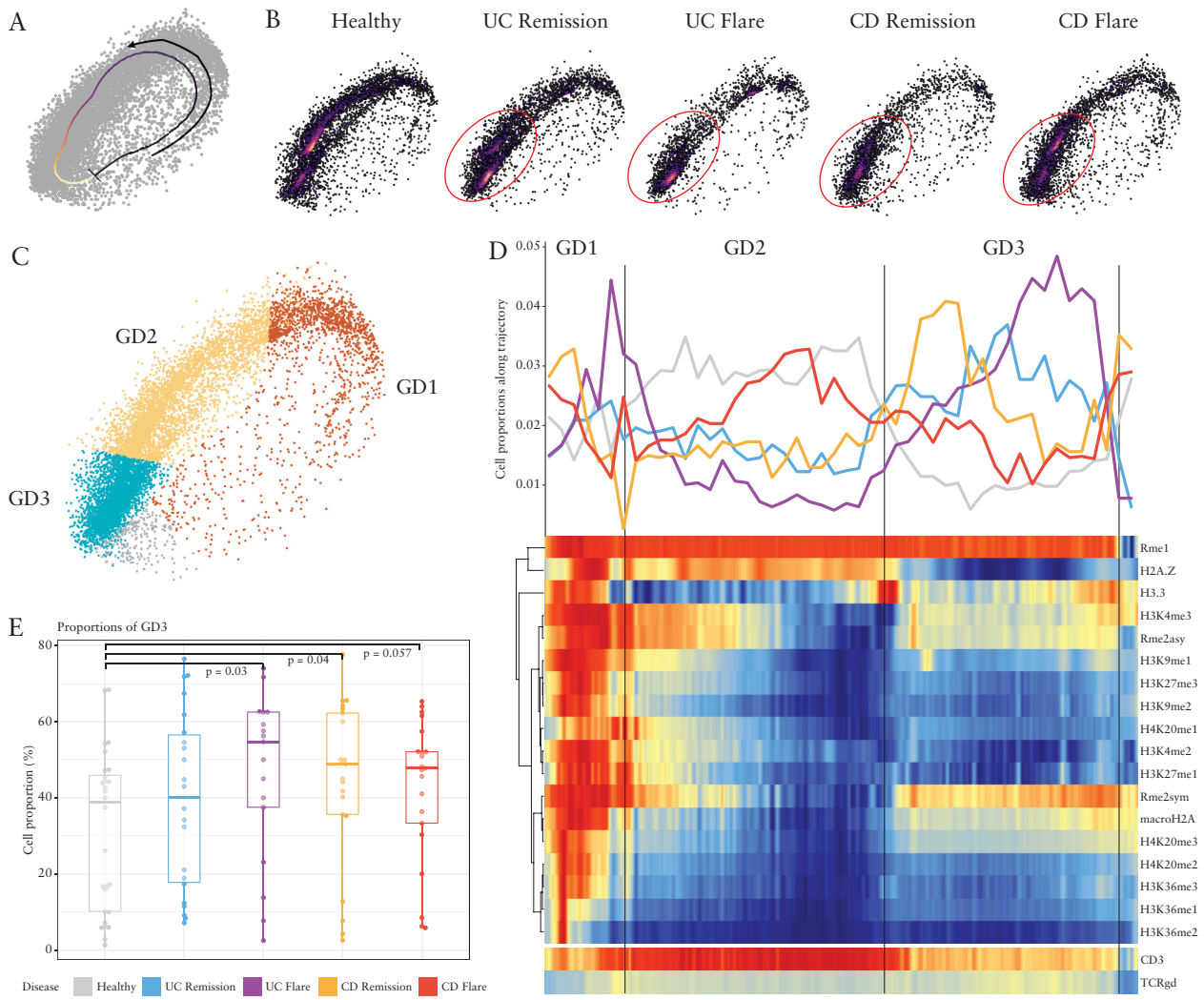


Figure 4. Epigenetic activation in γδT cells from patients with IBD. **[**A] tSpace trajectory analysis of EpiTOF histone modification abundance in γδT cells, separated by disease condition [B]. [C] Clustering of γδT cells along the tSpace trajectory. [D] Line plots of relative cell proportions between each disease condition along the linearized trajectory [top]; heatmap of histone modification abundance or cell surface marker expression across the linearized trajectory [bottom]. [E] Boxplot of GD3 cell proportions across disease conditions; Student's *t*-test.

acute inflammation and exist in an epigenetic state that supports active gene transcription.

We also observed a higher abundance of histone variants such as macroH2A and H3.3 in NK1 compared to other clusters. MacroH2A is a histone variant with a bulky C-terminal non-histone domain; previous studies have shown that macroH2A acts as an epigenetic barrier against induced pluripotency and chromatin plasticity.[49,50] H3.3 is a variant of the canonical H3, differing only by four to five amino acids. Despite this small structural difference, H3.3 impairs higher-ordered chromatin folding and promotes gene activation.[51]

Together, these results suggest that the proportion of specific subpopulations of NK cells, particularly the CD56^{bright} subset, is increased and has an epigenetically active phenotype under disease conditions.

3.5. γδT cells from patients with IBD demonstrated a histone modification environment supportive of active gene transcription

Given the conflicting reports on the role of γδ T cells in IBD,[52,53] we investigated the epigenetic landscape of γδ T cells. After applying tSpace, we found γδ T cells in IBD also formed a circular trajectory [Figure 4A]. Visual inspection of cell density along the trajectory suggested a shift in γδ T cells in patients with UC [Figure 4B]. After linearizing the trajectory, we identified three subclusters and calculated relative cell proportions in each subcluster [Figure 4C and D; see Methods]. A high abundance of almost all methylation markers defined cluster GD1, but cell proportions were equally present in healthy controls and patients with IBD, suggesting higher abundances of methylation markers per cell without changing the proportions of γδ T cells in the GD1 cluster.

In contrast, cluster GD3 contained a higher proportion of γδ T cells from patients with UC flare or CD compared to healthy controls [Figure 4D] and lower CD3 expression compared to GD2 [Figure 4E], which is in line with decreased expression of CD3 in γδ T cells from patients with IBD described previously.[53] TCR:CD3 complexes are downregulated during T cell activation across many acute and chronic diseases.[53,54] Notably, histone modifications or histone variants that were more abundant in activated NK cells were also more abundant in activated GD3 cells, including H3.3,

H3K4me3 and Rme2sym [Figure 4D]. Rme2asy, primarily mediated by *PRMT1*, was also upregulated in GD3. *PRMT1* is upregulated under inflammatory conditions and is involved in NF-κB regulation.[55] Together, our data suggest an increase in the proportion of γδ T cells in patients with IBD, especially during a flare, demonstrating a histone modification environment supportive of active gene transcription.

3.6 Classical monocytes from patients with IBD are epigenetically primed for macrophage differentiation

Evidence from multiple groups indicates a major role for inflammatory macrophages derived from peripheral CD34⁺ monocytes[56,57] in the pathology of IBD.[58–60] We recently demonstrated the regulatory role of cleaved H3T22 in determining the differentiation fate of monocytes into macrophages *in vitro*.[30] Circulating monocytes from patients with IBD had significantly lower cleaved H3T22 than healthy controls at the subject level [Supplementary Figure 9A]. This was in line with our previous study showing the same effects in systemic juvenile idiopathic arthritis [SJIA], another autoimmune disorder.[30] Together, these data suggest that peripheral CD34⁺ monocytes in patients with IBD are primed for macrophage differentiation and that cleaved H3T22 may provide an epigenetic link between monocytes, macrophages and IBD pathology.

3.7 Linear combination of cell cluster proportions derived from histone modifications distinguishes patients with IBD from healthy subjects

Finally, we investigated whether the proportions of HPCs, NK1 and GD3 could together distinguish patients with IBD from healthy controls. A logistic regression model with 5-fold cross-validation [see Methods] using proportions of these four immune cell subpopulations in each sample as features distinguished patients with IBD from healthy controls with an area under the receiver operating characteristic curve [AUROC] of 0.84 [95% confidence interval: 0.77–0.91; Figure 5], irrespective of disease subtype or severity [Supplementary Figure 9B]. The accuracy of our model was similar to other studies using whole exome genome sequencing[61] or combining serological, genetic and inflammatory markers.[62] Given that the input features of our model were cell proportions identified using histone modification abundances, our result suggests that epigenetics via histone modifications is strongly associated with IBD and may provide a novel pathway to explore disease pathology and pathogenesis.

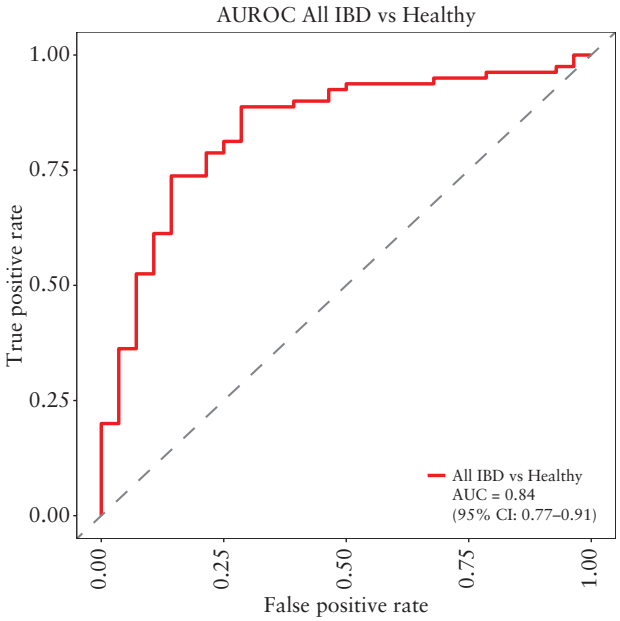


Figure 5. Cell cluster proportions derived from histone modifications distinguish patients with IBD from healthy subjects. Receiver operating curve [ROC] plot of the logistic regression method classifying patients with IBD versus healthy controls. AUC = 0.84; 95% CI = 0.77–0.91.

4. Discussion

Despite extensive progress in advancing the understanding of IBD pathology and developing novel therapies, there is still an unmet clinical need for long-lasting treatments. Part of the difficulty lies in the molecular heterogeneity observed in patients with IBD. With the growing evidence for the effectiveness of more personalized molecular classification of IBD,[63,64] it is increasingly important to investigate multiple facets of molecular pathways that can contribute to disease pathology.

Here, we performed the first systematic profiling of 38 histone modifications and histone variants in PBMCs from patients with IBD with or without flare and sought to address critical gaps in our knowledge. Using EpiTOF, we found that patients with IBD have a higher proportion of circulating immature CD34⁺ haematopoietic progenitors during an inflammatory flare. We also found subsets of NK cells and γδ T cells in patients with IBD, irrespective of disease subtype or severity, demonstrating histone modification environments supportive of active gene transcription associated with the high CRP in blood, and thus active IBD. We recently showed that cleaved H3T22 has a regulatory role in monocyte-to-macrophage differentiation and was decreased in patients with SJIA, another heterogeneous autoimmune inflammatory disease.[30] Interestingly, we also observed lower cleaved H3T22 in classical monocytes in patients with IBD. Importantly, cleaved H3T22 has not been widely studied regarding epigenetic regulation in the immune system, although cleaved H3T22 has been described in several species and processes.[65] Finally, our model using proportions of HPCs, NK1 and GD3 could distinguish patients with IBD from healthy controls. Overall, our study describes hitherto unreported epigenetic heterogeneity and changes in peripheral blood from patients with IBD.

Under inflammatory stress, innate immune cells are rapidly consumed at the site of need and thus must be replenished, a phenomenon known as emergency myelopoiesis.[66] Consequently, proliferative events lead to the early exit of immature progenitors into the bloodstream. An increase in proliferative haematopoietic stem cells in the bone marrow of IL-23-driven colitic mice has been reported, where subsequent inflammation led to skewed differentiation toward granulocyte-monocyte progenitors [GMPs].[67] Other studies have found that granulocyte-macrophage colony-stimulating factor [GM-CSF] is a critical modulator of intestinal macrophage activation and is primarily produced by innate lymphoid cell 3 [ILC3] in the intestine.[68–70] Our data are in line with these findings in patients with IBD. Furthermore, we recently reported the repression of controlled histone H3 amino terminus proteolytic cleavage [H3ΔN] during monocyte-to-macrophage development, which is catalysed by neutrophil

serine proteases [NSPs] cathepsin G [*CTSG*], neutrophil elastase [*ELANE*] and proteinase 3 [*PRTN3*].[30] Additionally, *in vitro* and *in vivo* studies are needed to evaluate the potential effects of targeting cleaved H3T22 proteases therapeutically.

CD56^{bright} NK cells are efficient producers of cytokines such as interferon γ [IFNγ], tumour necrosis factor α [TNFα] and GM-CSF.[44] Activated CD56^{bright} NK cells can promote TNFα production in CD34^{+} monocytes,[71] which have a well-established role in IBD pathology.[56,59] We found that patients with IBD have a larger proportion of CD56^{bright} NK cells, which suggests that a possible feedback mechanism exists through which these NK cells interact with pathogenic monocytes to drive further inflammation in patients with IBD. Further studies are warranted to confirm this cell–cell crosstalk and the exact mechanisms of action in the context of IBD. Our data suggest that γδ T cells in patients with IBD, demonstrating a histone modification environment supportive of active gene transcription, may contribute partly to IBD disease pathology. Combining our findings into a single classification model, we showed that four input features derived from epigenetic subsets of immune cell types could accurately classify patients with IBD from healthy samples, irrespective of disease subtype or severity. Collectively, this suggests that epigenetics, particularly histone modifications, play a crucial role in the context of IBD pathology.

4.1. Limitations of the study

Our analysis has several limitations. First, despite parallelizing the measurement of multiple cell types and epigenetic marks, EpiTOF does not provide locus-specific histone modifications. Hence, further experiments, including ChIP-seq or cut&run of specific cell type–marker pairs, are required to uncover transcriptional alterations at the genome level. Second, none of the patients we used were treatment-naïve. However, it is essential to note that since most patients in academic and/or tertiary centres are not treatment-naive, our cohort reflects 'real-world' patients encountered in most clinical settings. Third, our study does not have sufficient statistical power to investigate the association between epigenetic changes and patients' treatments. Targeted studies that will recruit patients with specific therapies are more fit to provide insight into the effects of treatments on epigenetic modifications. Fourth, the accuracy of our logistic regression model to distinguish patients with IBD from healthy controls needs to be validated in an independent cohort. Overall, future studies will address the limitations of this work, including subsequent experiments to identify specific genome-wide peaks that are significantly changed in the context of disease. For example, ChIP-seq on several epigenetic marks of interest shared between NK cells and γδ T cells may yield specific genes that are accessible or active during disease flare.

Funding

LB is funded by the Stanford Bio-X Graduate Fellowship. PK is funded by the Bill and Melinda Gates Foundation [OPP1113682]; the National Institute of Allergy and Infectious Diseases [NIAID] grants 1U19AI167903-01, 5U01AI165527-02, 1U19AI109662, U19AI057229 and 5R01AI125197; Department of Defense contracts W81XWH-18-1-0253 and W81XWH1910235; and the Ralph & Marian Falk Medical Research Trust.

Conflict of Interest

The authors report no conflicts of interest.

Acknowledgments

The authors thank T. Balabanis, A. Patel, S. Toppo and A. Sharma for clinical and technical assistance in recruiting patients and isolating PBMCs; Y. Wei, Y. Yang, A. Ji and D. Mikhail for technical assistance; S. J. S. Rubin, A. Fan, G. Swaminathan and B. Lee for technical help with experimental design; and the patients and healthcare providers without whom this study would not have been possible.

Author Contributions

LB, AH and PK conceived the study. LB, DD and PK interpreted data. LB, DD and PK wrote the manuscript. LB designed the cohorts, and acquired, processed and analysed the single-cell data. MDv and SEC processed samples and performed the EpiTOF profiling. MDo, DD, LK and AG developed methods for the analysis of EpTOF, and advised, and assisted in data analyses and interpretation. AH advised regarding clinical relevance and edited the manuscript. All authors reviewed and edited the manuscript. PK supervised the project.

Ethics Statement

All blood samples were collected using a study protocol approved by the Stanford Institutional Review Board [IRB-28427]. Informed consent was obtained from all subjects and healthy controls in this study.

Data Availability Statement

All EpiTOF data in this paper are publicly available for use at https://khatrilab.stanford.edu/epitof/.

Supplementary Data

Supplementary data are available online at *ECCO-JCC* online.

References

1. Abraham C, Cho JH. Inflammatory bowel disease. *N Engl J Med* 2009;**361**:2066–78.
2. GBD 2017 Inflammatory Bowel Disease Collaborators. The global, regional, and national burden of inflammatory bowel disease in 195 countries and territories, 1990–2017: a systematic analysis for the Global Burden of Disease Study 2017. *Lancet Gastroenterol Hepatol* 2019;**5**:17–30.
3. Ungaro R, Mehandru S, Allen PB, Peyrin-Biroulet L, Colombel JF. Ulcerative colitis. *Lancet* 2017;**389**:1756–70.
4. Baumgart DC, Carding SR. Inflammatory bowel disease: cause and immunobiology. *Lancet* 2007;**369**:1627–40.
5. Cosnes J, Gower–Rousseau C, Seksik P, Cortot A. Epidemiology and natural history of inflammatory bowel diseases. *Gastroenterology* 2011;**140**:1785–1794.e4.
6. Kaplan GG. The global burden of IBD: from 2015 to 2025. *Nat Rev Gastroenterol* 2015;**12**:720–7.
7. Loddo I, Romano C. Inflammatory bowel disease: genetics, epigenetics, and pathogenesis. *Front Immunol* 2015;**6**:551.

8. Santos MPC, Gomes C, Torres J. Familial and ethnic risk in inflammatory bowel disease. *Ann Gastroenterol* 2018;**31**:14–23.
9. Jostins L, Ripke S, Weersma RK, *et al*; International IBD Genetics Consortium (IIBDGC). Host–microbe interactions have shaped the genetic architecture of inflammatory bowel disease. *Nature* 2012;**491**:119–24.
10. Ananthakrishnan AN, *et al*. Environmental triggers in IBD: a review of progress and evidence. *Nat Rev Gastroenterol* 2018;**15**: 39–49.
11. Allis CD, Jenuwein T. The molecular hallmarks of epigenetic control. *Nat Rev Genet* 2016;**17**:487–500.
12. Zhang Y, Kutateladze TG. Diet and the epigenome. *Nat Commun* 2018;**9**:3375.
13. Zong D, Liu X, Li J, Ouyang R, Chen P. The role of cigarette smoke-induced epigenetic alterations in inflammation. *Epigenet Chromatin* 2019;**12**:65.
14. Renz H, von Mutius E, Brandtzaeg P, Cookson WO, Autenrieth IB, Haller D. Gene–environment interactions in chronic inflammatory disease. *Nat Immunol* 2011;**12**:273–7.
15. Ventham NT, Kennedy NA, Nimmo ER, Satsangi J. Beyond gene discovery in inflammatory bowel disease: the emerging role of epigenetics. *Gastroenterology* 2013;**145**:293–308.
16. Ray G, Longworth MS. Epigenetics, DNA organization, and inflammatory bowel disease. *Inflamm Bowel Dis* 2019;**25**: 235–47.
17. Tahara T, Shibata T, Nakamura M, *et al*. Effect of MDR1 gene promoter methylation in patients with ulcerative colitis. *Int J Mol Med* 2009;**23**:521–7.
18. Cooke J, Zhang H, Greger L, *et al*. Mucosal genome-wide methylation changes in inflammatory bowel disease. *Inflamm Bowel Dis* 2012;**18**:2128–37.
19. Howell KJ, Kraiczy J, Nayak KM, *et al*. DNA methylation and transcription patterns in intestinal epithelial cells from pediatric patients with inflammatory bowel diseases differentiate disease subtypes and associate with outcome. *Gastroenterology* 2018;**154**:585–98.
20. Kalla R, Adams AT, Satsangi J. Blood-based DNA methylation in Crohn's disease and severity of intestinal inflammation. *Transl Gastroenterol Hepatol* 2019;**4**:76.
21. Tsaprouni LG, Ito K, Powell JJ, Adcock IM, Punchard N. Differential patterns of histone acetylation in inflammatory bowel diseases. *J Inflamm Lond Engl* 2011;**8**:1.
22. Sarmento OF, Svingen PA, Xiong Y, *et al*. The role of the histone methyltransferase Enhancer of Zeste Homolog 2 (EZH2) in the pathobiological mechanisms underlying inflammatory bowel disease [IBD]. *J Biol Chem* 2017;**292**:706–22.
23. Kelly D, Kotliar M, Woo V, *et al*. Microbiota-sensitive epigenetic signature predicts inflammation in Crohn's disease. *JCI Insight* 2018;**3**:e122104.
24. Wu F, Zikusoka M, Trindade A, *et al*. MicroRNAs are differentially expressed in ulcerative colitis and alter expression of macrophage inflammatory peptide-2 alpha. *Gastroenterology* 2008;**135**:1624–1635.e24.
25. Wu F, Zhang S, Dassopoulos T, *et al*. Identification of microRNAs associated with ileal and colonic Crohn's disease. *Inflamm Bowel Dis* 2010;**16**:1729–38.
26. Bai AHC, Wu WKK, Xu L, *et al*. Dysregulated lysine acetyltransferase 2B promotes inflammatory bowel disease pathogenesis through transcriptional repression of interleukin-10. *J Crohns Colitis* 2016;**10**:726–34.
27. Liu T, Wang R, Xu H, Song Y, Qi Y. A Highly potent and selective histone deacetylase 6 inhibitor prevents DSS-induced colitis in mice. *Biol Pharm Bull* 2017;**40**:b16–01023.
28. Cheung P, Vallania F, Warsinske HC, *et al*. Single-cell chromatin modification profiling reveals increased epigenetic variations with aging. *Cell* 2018;**173**:1385–1397.e14.
29. Dermadi D, *et al*. Exploration of cell development pathways through high dimensional single cell analysis in trajectory space. *Biorxiv* 2018;336313. doi:10.1101/336313.
30. Cheung P, Schaffert S, Chang SE, *et al*. Repression of CTSG, ELANE and PRTN3-mediated histone H3 proteolytic cleavage promotes monocyte-to-macrophage differentiation. *Nat Immunol* 2021;**22**:711–22.
31. Vallania F, *et al*. Leveraging heterogeneity across multiple datasets increases cell-mixture deconvolution accuracy and reduces biological and technical biases. *Nat Commun* 2018;**9**:4735.
32. Haynes WA, *et al*. Empowering multi-cohort gene expression analysis to increase reproducibility. *Pac Symposium Biocom put*2016;**22**:144–53.
33. Dermadi D, *et al*. Exploration of cell development pathways through high-dimensional single cell analysis in trajectory space. *Iscience* 2019;**23**:100842.
34. Wimmers F, Donato M, Kuo A, *et al*. The single-cell epigenomic and transcriptional landscape of immunity to influenza vaccination. *Cell* 2021;**184**:3915–3935.e21.
35. McInnes L, Healy J, Melville J. UMAP: Uniform manifold approximation and projection for dimension reduction. *Arxiv* 2018 doi:10.48550/arxiv.1802.03426.
36. Levine JH, Simonds EF, Bendall SC, *et al*. Data-driven phenotypic dissection of AML reveals progenitor-like cells that correlate with prognosis. *Cell* 2015;**162**:184–97.
37. Urdinguio RG, Lopez V, Bayón GF, *et al*. Chromatin regulation by Histone H4 acetylation at Lysine 16 during cell death and differentiation in the myeloid compartment. *Nucleic Acids Res* 2019;**47**:5016–37.
38. Sheikh BN, *et al*. MOZ (KAT6A) is essential for the maintenance of classically defined adult hematopoietic stem cells. *Blood* 2015;**128**:2307–18.
39. MacPherson L, Anokye J, Yeung MM, *et al*. HBO1 is required for the maintenance of leukaemia stem cells. *Nature* 2020;**577**:266–70.
40. Chen X, *et al*. G9a/GLP-dependent histone H3K9me2 patterning during human hematopoietic stem cell lineage commitment. *Gene Dev* 2012;**26**:2499–511.
41. Zhu L, He X, Dong H, *et al*. Protein arginine methyltransferase 1 is required for maintenance of normal adult hematopoiesis. *Int J Biol Sci* 2019;**15**:2763–73.
42. Liu F, Cheng G, Hamard P-J, *et al*. Arginine methyltransferase PRMT5 is essential for sustaining normal adult hematopoiesis. *J Clin Invest* 2015;**125**:3532–44.
43. Poli A, Michel T, Thérésine M, Andrès E, Hentges F, Zimmer J. CD56bright natural killer (NK) cells: an important NK cell subset. *Immunology* 2009;**126**:458–65.
44. Barski A, Cuddapah S, Cui K, *et al*. High-resolution profiling of histone methylations in the human genome. *Cell* 2007;**129**:823–37.
45. Zaghi M, Broccoli V, Sessa A. H3K36 methylation in neural development and associated diseases. *Front Genet* 2020;**10**:1291.
46. Wagner EJ, Carpenter PB. Understanding the language of Lys36 methylation at histone H3. *Nat Rev Mol Cell Biol* 2012;**13**: 115–26.
47. Inoue M, Okamoto K, Terashima A, *et al*. Arginine methylation controls the strength of γc-family cytokine signaling in T cell maintenance. *Nat Immunol* 2018;**19**:1265–76.
48. Metz PJ, Ching KA, Xie T, *et al*. Symmetric arginine dimethylation is selectively required for mRNA Splicing and the initiation of type I and type III interferon signaling. *Cell Rep* 2020;**30**:1935–1950.e8.
49. Gaspar-Maia A, Qadeer ZA, Hasson D, *et al*. MacroH2A histone variants act as a barrier upon reprogramming towards pluripotency. *Nat Commun* 2013;**4**:1565–1565.
50. Kozlowski M, *et al*. MacroH2A histone variants limit chromatin plasticity through two distinct mechanisms. *EMBO Rep* 2018;**19**.
51. Chen P, *et al*. H3.3 actively marks enhancers and primes gene transcription via opening higher-ordered chromatin. *Gene Dev* 2013;**27**:2109–24.
52. Kühl AA, Loddenkemper C, Westermann J, Hoffmann JC. Role of gamma delta T cells in inflammatory bowel disease. *Pathobiology* 2003;**70**:150–5.

53. Mann ER, McCarthy NE, Peake STC, *et al*. Skin- and gut-homing molecules on human circulating γδ T cells and their dysregulation in inflammatory bowel disease. *Clin Exp Immunol* 2012;**170**: 122–30.
54. Liu H, Rhodes M, Wiest DL, Vignali DAA. On the dynamics of TCR:CD3 complex cell surface expression and downmodulation. *Immunity* 2000;**13**:665–75.
55. Kim JH, *et al*. The role of protein arginine methyltransferases in inflammatory responses. *Mediat Inflamm* 2016;**2016**:4028353.
56. Grimm M, *et al*. Direct evidence of monocyte recruitment to inflammatory bowel disease mucosa. *J Gastroenterol Hepatol* 1995;**10**:387–95.
57. Caër C, Wick MJ. Human intestinal mononuclear phagocytes in health and inflammatory bowel disease. *Front Immunol* 2020;**11**:410.
58. Kamada N, *et al*. Unique CD14 intestinal macrophages contribute to the pathogenesis of Crohn disease via IL-23/IFN-gamma axis. *J Clin Invest* 2007;**118**:2269–80.
59. Lissner D, Schumann M, Batra A, *et al*. Monocyte and M1 macrophage-induced barrier defect contributes to chronic intestinal inflammation in IBD. *Inflamm Bowel Dis* 2015;**21**:1297–305.
60. Thiesen S, *et al*. CD14(hi)HLA-DR(dim) macrophages, with a resemblance to classical blood monocytes, dominate inflamed mucosa in Crohn's disease. *J Leukocyte Biol* 2013;**95**:531–41.
61. Jeong C-S, Kim D. Inferring Crohn's disease association from exome sequences by integrating biological knowledge. *BMC Med Genomics* 2016;**9**:35.
62. Plevy S, Silverberg MS, Lockton S, *et al*. Combined serological, genetic, and inflammatory markers differentiate non-IBD, crohn's disease, and ulcerative colitis patients. *Inflamm Bowel Dis* 2013;**19**:1139–48.
63. Weiser M, *et al*. Molecular classification of Crohn's disease reveals two clinically relevant subtypes. *Gut* 2018;**67**:36-42.
64. Potdar AA, *et al*. Ileal gene expression data from crohn's disease small bowel resections indicate distinct clinical subgroups. *J Crohns Colitis* 2019;**13**:1055–66.
65. Kragesteen BK, Amit I. Heads or tails: histone tail clipping regulates macrophage activity. *Nat Immunol* 2021;**22**:678–80.
66. Takizawa H, Boettcher S, Manz MG. Demand-adapted regulation of early hematopoiesis in infection and inflammation. *Blood* 2012;**119**:2991–3002.
67. Griseri T, McKenzie BS, Schiering C, Powrie F. Dysregulated hematopoietic stem and progenitor cell activity promotes interleukin-23-driven chronic intestinal inflammation. *Immunity* 2012;**37**:1116–29.
68. Pearson C, Thornton EE, McKenzie B, *et al*. ILC3 GM-CSF production and mobilisation orchestrate acute intestinal inflammation. *Elife* 2016;**5**:e10066.
69. Castro-Dopico T, *et al*. GM-CSF calibrates macrophage defense and wound healing programs during intestinal infection and inflammation. *Cell Rep* 2020;**32**:107857.
70. Regan-Komito D, *et al*. GM-CSF drives dysregulated hematopoietic stem cell activity and pathogenic extramedullary myelopoiesis in experimental spondyloarthritis. *Nat Commun* 2020;**11**:155
.
71. Dalbeth N, Gundle R, Davies RJO, Lee YCG, McMichael AJ, Callan MFC. CD56bright NK cells are enriched at inflammatory sites and can engage with monocytes in a reciprocal program of activation. *J Immunol* 2004;**173**:6418–26.